Cardiomyocyte Cultures With Controlled Macroscopic Anisotropy: A Model for Functional Electrophysiological Studies of Cardiac Muscle

N. Bursac, K.K. Parker, S. Iravanian and L. Tung

Circ. Res. 2002;91;e45-e54; originally published online Nov 14, 2002;
DOI: 10.1161/01.RES.0000047530.88338.EB
Circulation Research is published by the American Heart Association. 7272 Greenville Avenue, Dallas, TX 72514
 Print ISSN: 0009-7330. Online ISSN: 1524-4571

UltraRapid Communication

Cardiomyocyte Cultures With Controlled Macroscopic Anisotropy

A Model for Functional Electrophysiological Studies of Cardiac Muscle

N. Bursac, K.K. Parker, S. Iravanian, L. Tung

Abstract—Structural and functional cardiac anisotropy varies with the development, location, and pathophysiology in the heart. The goal of this study was to design a cell culture model system in which the degree, change in fiber direction, and discontinuity of anisotropy can be controlled over centimeter-size length scales. Neonatal rat ventricular myocytes were cultured on fibronectin on 20-mm diameter circular cover slips. Structure-function relationships were assessed using immunostaining and optical mapping. Cell culture on microabraded cover slips yielded cell elongation and coalignment in the direction of abrasion, and uniform, macroscopically continuous, elliptical propagation with point stimulation. Coarser microabrasion (wider and deeper abrasion grooves) increased longitudinal (23.5 to 37.2 cm/s; $r=0.66$) and decreased transverse conduction velocity (18.1 to 9.2 cm/s; $r=-0.84$), which resulted in increased longitudinal-to-transverse velocity anisotropy ratios (1.3 to 3.7, n=61). A thin transition zone between adjacent uniformly anisotropic areas with 45° or 90° difference in fiber orientation acted as a secondary source during 2× threshold field stimulus. Cell culture on cover slips micropatterned with 12- or 25-μm wide fibronectin lines and previously coated with decreasing concentrations of background fibronectin yielded transition from continuous to discontinuous anisotropic architecture with longitudinally oriented intercellular clefts, decreased transverse velocity (16.9 to 2.6 cm/s; $r=-0.95$), increased velocity anisotropy ratios (1.6 to 5.6, n=70), and decreased longitudinal velocity (36.4 to 14.6 cm/s; $r=-0.85$) for anisotropy ratios >3.5. Cultures of cardiac myocytes with controlled degree, uniformity and continuity of structural, and functional anisotropy may enable systematic 2-dimensional in vitro studies of macroscopic structure-related mechanisms of reentrant arrhythmias. The full text of this article is available at http://www.circresaha.org. **(*Circ Res*. 2002;91:e45-e54.)**

Key Words: anisotropy ■ cardiac electrophysiology ■ optical mapping ■ cell culture

Anatomically and biophysically, cardiac tissue is anisotropic; ie, properties of cardiac muscle vary according to the direction of measurement. Microscopic anatomical anisotropy results from the spatial alignment of elongated cardiac myocytes, and/or the preferential location of intercellular junctions (eg, fascia adherens, gap junctions, and desmosomes) in end-to-end versus side-to-side cell connections.[1] Macroscopic anatomical anisotropy is a consequence of the formation of cardiac muscle fibers and bundles that rotate transmurally inside the heart. The unique anisotropic architecture of cardiac tissue enables an orderly sequence of electrical and mechanical activity and efficient pumping of blood from the heart.

Anisotropy and continuity of the excitable substrate has a profound effect on impulse initiation and propagation. For example, anatomical anisotropy in heart tissue causes a larger cellular coupling resistance in the transverse (along short cell axis) than longitudinal (along long cell axis) direction, resulting in a smaller velocity but larger maximum slope of action potential upstroke and safety factor of impulse propagation in the transverse direction. The presence of resistive discontinuities and anisotropy in cardiac tissue is also believed to dictate the formation and spatial distribution of virtual sources during electrical stimulation,[2] which is of particular importance in understanding mechanisms of defibrillation.[3]

The degree of anatomical and functional anisotropy depends on location in the heart and age of the individual,[4,5] with main determinants being type, amount, and distribution of gap junctions in the cell membrane, cell size and geometry, and tissue architecture.[1,6] In addition, sharp changes in fiber direction throughout the heart appear to play an important role in wave splitting and maintenance of cardiac fibrillation.[7] Anisotropy also changes in certain cardiac pathologies such

Original received September 6, 2002; revision received October 22, 2002; accepted November 5, 2002.
From the Department of Biomedical Engineering, The Johns Hopkins University, Baltimore, Md.
This manuscript was sent to Michael R. Rosen, Consulting Editor, for review by expert referees, editorial decision, and final disposition.
Presented in part at the Biomedical Engineering Society Annual Meeting, Durham, NC, October 4–7, 2001, and published in abstract form (*Ann Biomed Eng*. 2001;29[suppl 1]:S-52) and at the North American Society of Pacing and Electrophysiology 23rd Annual Scientific Sessions, San Diego, Calif, May 8–11, 2002, and published in abstract form (*PACE*. 2002;25:578).
Correspondence to Dr Leslie Tung, Dept of Biomedical Engineering, Johns Hopkins University, 720 Rutland Ave, Baltimore, MD 21205. E-mail ltung@bme.jhu.edu

Circulation Research **is available at http://www.circresaha.org** **DOI: 10.1161/01.RES.0000047530.88338.EB**

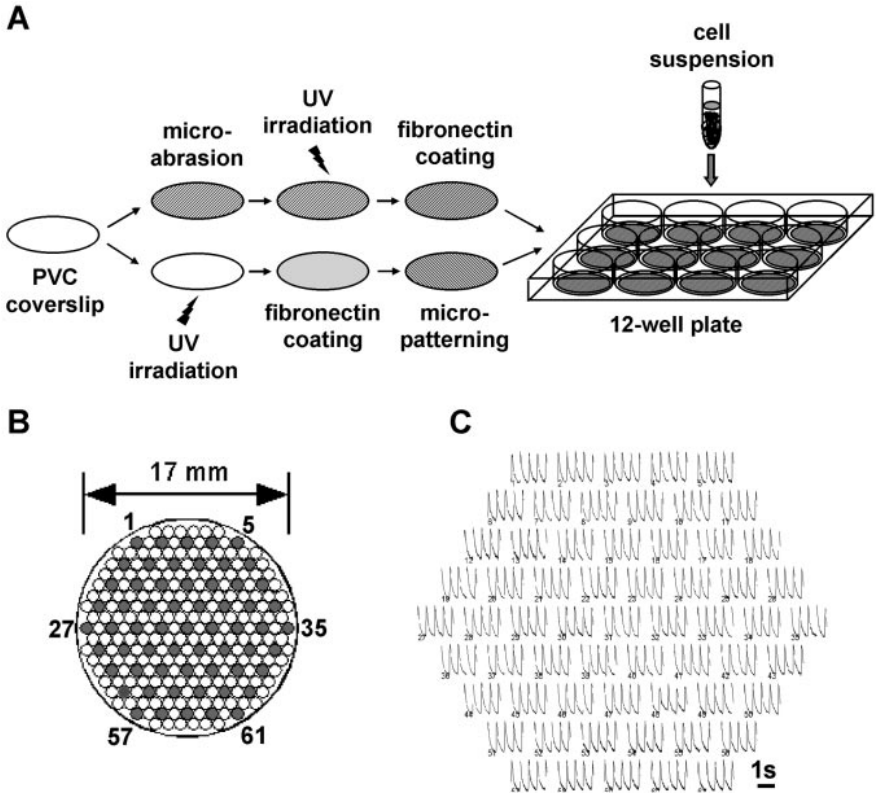

Figure 1. A, Preparation of culture substrate. Circular polyvinyl chloride (PVC) cover slips (20-mm diameter) were (1) microabraded, UV irradiated, and fibronectin coated, or (2) UV irradiated, fibronectin coated, and micropatterned, plated with 7.5×10^5 neonatal rat cardiac cells per cover slip, and cultured for 5 to 7 days. B, Fiber-optic bundle for optical mapping of electrical propagation. Gray circles (marked 1 to 61) represent recording sites spaced 2 mm apart. C, Optically recorded action potentials traces during 2-Hz point pacing at the center of the culture.

as ischemia, infarction, and heart failure.[8,9] This change is a consequence of the altered gap junction distribution and/or expression, as well as formation of collagenous septa between the cardiac fibers and groups of cells that result in discontinuous transverse propagation ("nonuniform anisotropy").[5] Remodeling of cardiac anisotropy, as in the case of the canine model of infarction,[9] may play an important role in the production of conduction abnormalities that generate reentrant circuits in the heart. In general, lack of knowledge about the relationship between different anatomic substrates and electrical propagation demands new experimental modalities, which can provide simple, reproducible, well-controlled environments for rigorous theoretical and experimental analysis of conduction at the cellular and tissue levels.

In previous studies, different dissection or cryoablation techniques[10–13] have been applied to study impulse propagation in a simplified setting of thin (practically 2-dimensional) cardiac sheets instead of the complex 3-dimensional wall of the intact heart. Moreover, micropatterned cell monolayers in conjunction with high-resolution optical mapping have provided valuable insights of the role of tissue microstructure on excitation and wavefront propagation at subcellular to millimeter-size length scales.[14–17] In our previous study, we introduced the technique of contact fluorescence imaging to record transmembrane potentials and electrical propagation in cardiac cell cultures at a macroscopic (centimeter-sized) scale.[18] The goal of this study was to design an in vitro model system for controlled studies of structure-related phenomena in cardiac muscle by systematic manipulation of macroscopic tissue architecture in cardiac cell cultures. Methods of microabrasion and micropatterning were developed in cardiac cell cultures to control (1) the degree of anisotropy, (2) fiber direction, and (3) continuity of anisotropy (discontinuous propagation in transverse direction). Immunostaining and fluorescence microscopy were used to evaluate architecture of the monolayer cultures, whereas optical mapping and programmed pacing were used to assess macroscopic wavefront propagation. Cultures of cardiac myocytes with defined and reproducible architecture at the macroscopic length scale represent a promising tool for electrophysiological, pharmacological, and genetic studies of impulse propagation and reentry dynamics in a 2-dimensional in vitro setting.

Materials and Methods

All animals were treated according to protocols approved by the Animal Use and Care Committee at the Johns Hopkins University School of Medicine.

Cell Culture

Cardiac cells were dissociated from ventricles of 2- to 3-day old neonatal Sprague-Dawley rats (Harlan, Indianapolis, Ind) using trypsin (US Biochemicals) and collagenase (Worthington) and resuspended in culture medium supplemented with 10% FBS, as previously described.[19]

Microabrasion

Polyvinyl chloride (PVC) cover slips (22×22 mm^2; PGC Scientifics, Frederick, Md) were microabraded (1) over the entire surface in a direction parallel to one of the edges using lapping papers with different grit sizes (McMaster-Corr) to produce uniformly anisotropic cultures with varying degrees of anisotropy, or (2) at two different directions in two adjacent regions to form anisotropic cultures with sharp change in fiber direction. Abraded cover slips were cut into a circular shape (≈20-mm diameter) to fit wells of a standard 12-well tissue culture plate (Figure 1A), thoroughly rinsed in 95% ethanol, dried using pressurized nitrogen, UV irradiated for 1.5 hours to make the PVC surface more hydrophilic, and coated with fibronectin (25 μg/mL in PBS) at room temperature for 2 hours.

To assess if microabraded cover slips can be reused for culture, three cover slips (each microabraded with different coarseness) were reused and assessed in four independent experiments each. Between experiments, cover slips were washed in deionized water, sonicated for 15 minutes in 70% ethanol, and on the day of culture rinsed in 95% ethanol, dried using pressurized nitrogen, UV irradiated for 30 minutes, and fibronectin-coated as described above.

Micropatterning

Cover slips (22×22 mm^2) were cut into a circular shape (≈20 mm diameter) and micropatterned over the entire surface with 12- or 25-μm parallel, equally spaced (12- and 25-μm spacing, respectively) fibronectin lines using modified microcontact printing techniques.[20,21] Briefly, lines of photoresist were micropatterned on 30-mm circular glass cover slips using standard photolithography techniques with a photomask made of Ronchi ruling glass (Edmund Industrial Optics). Polydimethylsiloxane (PDMS) (Sylgard 184, Dow Corning) stamps were then cast against the micropatterned glass cover slips overnight at 65°C. Stamps were cut to 20×20 mm^2, covered with 50 μg/mL of fibronectin in PBS for 1.5 hours at room temperature, rinsed, dried using pressurized nitrogen, and pressed against the 20-mm cover slips for 30 minutes to transfer the protein lines. The PVC cover slips were cleaned previously and either not treated with UV light, or UV treated for 1 hour and coated for 2 hours with 1.25, 2.5, or 5 μg/mL of fibronectin in PBS. The pretreatment with varying background concentrations of fibronectin was used to control the amount of transverse connections (nonuniform discontinuous anisotropy) between the patterned cells. PDMS stamps could be reused up to 5 times if sonicated in 70% ethanol for 30 minutes between different cultivations.

Microabraded, micropatterned, and unmodified (control) cover slips were plated with 7.5×10^5 cells (Figure 1A). At 2 days after cell plating, serum was reduced to 2%. At days 5 to 7, cultures were assessed for morphology and function.

Scanning Electron Microscopy

Scanning electron micrographs of abraded PVC cover slips were used to evaluate the degree and uniformity of surface microabrasion. Abraded cover slips were frozen in liquid nitrogen, broken prior to drying in high vacuum, and coated with a 20-nm layer of gold. Images were acquired using a scanning electron microscope (LEO 1550 FESEM, LEO-EM).

Immunofluorescence

Light micrographs and immunofluorescent staining were used to assess cell type, density, coalignment, gross ultrastructure, and intercellular connections. Fibronectin, actin, sarcomeric α-actinin, and nuclear DNA in paraformaldehyde-fixed cells were visualized with fluorescence microscopy using rabbit anti-fibronectin antibody, fluorescein-conjugated phalloidin, mouse anti–α-actinin antibody, and DAPI staining (all from Sigma, with secondary antibodies from Molecular Probes), as previously described.[22] Immunostaining of gap junction protein connexin-43 (primary antibody from Chemicon International) required a modification of this protocol, where cells were fixed in 2% paraformaldehyde for 4 minutes during permeabilization and before incubation with the primary antibody.

Electrophysiological Recording

For the formation of uniformly anisotropic cultures, special care was taken that monolayers had no anatomical discontinuity caused by under-confluence of cells. Before recording, cell cultures were carefully assessed under the microscope, and discarded (10% rate) if not fully confluent. For electrophysiological recordings, cover slips with cell monolayers were equilibrated in warmed (T=35±0.5°C) oxygenated Tyrode's solution (in mmol/L: 135 NaCl, 5.4 KCl, 1.8 $CaCl_2$, 1 $MgCl_2$, 0.33 NaH_2PO_4, 5 HEPES, 5 glucose) in a custom designed chamber for 5 to 10 minutes, stained with RH-237 voltage-sensitive dye (Molecular Probes) for 5 minutes, and continuously superfused afterward. A plexiglas cover was placed on top of the chamber to stabilize the surface of the solution and reduce optical artifacts.

Experimental Protocol

After staining, cultures were equilibrated for at least 5 minutes, and a 3-second recording was made in the absence of electrical stimulation to check for spontaneous activity. Only cultures with spontaneous rates less than 2 Hz (≈90% of total number of cultures) were used for the experiments. Cathodal point stimuli (1.2× threshold, 10 ms duration) were applied at a rate of 2 Hz using the tip of a 100-μm diameter platinum wire placed ≈1 mm above the culture surface at various locations, with a platinum foil return electrode fixed in the bath >6 mm away from the cover slip. A cell monolayer was excluded from the experiment if either (1) two or more adjacent recording points showed no sign of an action potential, or (2) a gross discontinuity or deformation was observed in the isochrone map of the convex spread of activity generated by point stimulation. Based on the criteria above, 155 (80 microabraded and 75 micropatterned) out of 175 cover slips were considered for this study. The cultures with sharp change in fiber direction were also field stimulated at 3 to 13 V/cm using 2 parallel rectangular (33×4 mm) platinum foil

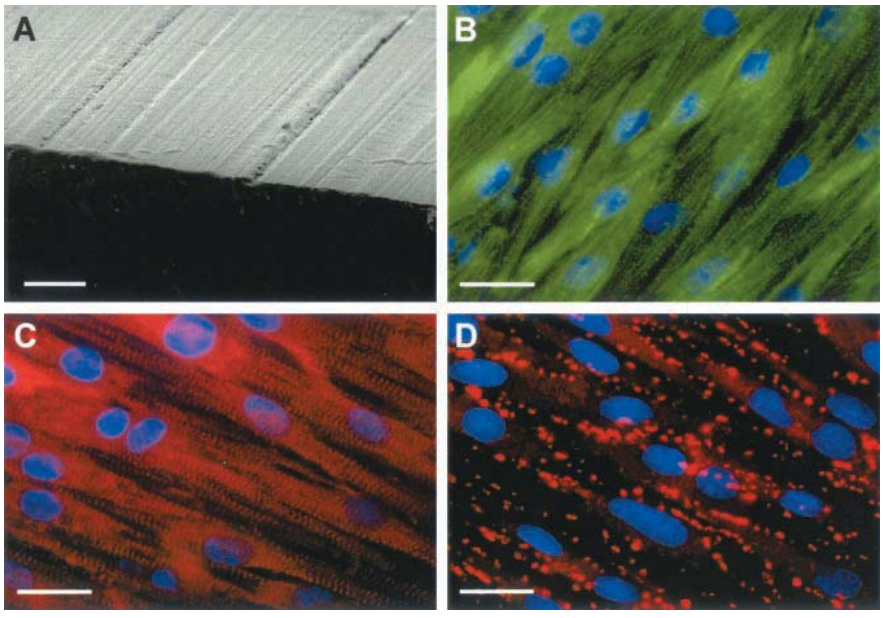

Figure 2. Cardiac cell morphology in confluent anisotropic cultures produced by microabrasion. A, Scanning electron micrograph of an edge of a microabraded PVC cover slip using lapping paper of medium coarseness. Bar=10 μm. Architecture of elongated and coaligned cells shown by green staining for actin (B), red staining for sarcomeric α-actinin (C), and red staining for connexin43 (D). Cell nuclei are shown in blue. B through D, Bars=25 μm.

electrodes, which covered the opposite walls of the recording chamber.

Action potentials were optically recorded from 61 sites using a modification of the contact fluorescence imaging (CFI) method.[18] Briefly, the recording chamber was placed directly above a fiber optic bundle arranged in a 17-mm diameter hexagonal array (Figure 1B). Cultures were illuminated with green excitation light (530±25 nm), and optical responses were filtered through red ink (Avery Dennison) painted on the bottom of the chamber and the front end of the fiber bundle. Signals were converted to voltage, sampled at 1 kHz, stored, displayed (Figure 1C), and analyzed using software written in Visual Basic (Microsoft Corp) and Matlab (Mathworks Inc).

Data Analysis

Linear baseline drift was nullified by first fitting a straight line to and then subtracting it from the recorded data. The activation time was defined as the instant of maximum positive slope of the action potential. Velocity fields were calculated from inverse gradients of isochrone maps, similar to previous methods.[23] Longitudinal (LCV) and transverse (TCV) conduction velocities during point stimulation were obtained by averaging the velocity magnitude along the major and minor axes of elliptical isochrones, respectively, at sites at least 4 mm away from the stimulation point. The same sites were used to measure longitudinal and transverse action potential duration at 80% repolarization ($APD_{80,L}$ and $APD_{80,T}$). APD_{80} was defined as the interval from activation time to 80% repolarization of the action potential. The longitudinal and transverse wavelengths (λ_L and λ_T) for the point-stimulated excitation wave were calculated using the generic expression $\lambda = APD_{80} \cdot CV$. Anisotropy velocity ratio (AR) was defined as AR=LCV/TCV.

Statistical Analysis

Data were expressed as mean±SD and analyzed using one-way ANOVA followed by post hoc Student's *t* test. Correlation and regression analysis (Excel, Microsoft) were used to evaluate trends in the data sets. Differences were considered to be significant when $P<0.05$.

Results

Microabrasion

According to the manufacturer specifications, the abrasive SiC_4 crystal heads that were embedded in the lapping paper had average diameters ranging from 0.5 to 14 μm. We classified lapping papers in the low (0.5 and 1 μm), middle (6 μm), and high (14 μm) diameter range as fine, medium, and coarse. Scanning electron micrographs (SEMs) from the center and the edge (Figure 2A) revealed that microabrasion produced thin, parallel grooves (lines) that ran at approximately uniform density throughout the cover slip. Coarser abrasion produced wider and deeper lines with average line width and depth of approximately 0.5 and 0.2, 2 and 1, and 5 and 2 μm for fine, medium, and coarse abrasion, respectively, as estimated from SEMs.

After cultivation for 5 to 7 days, cardiac cells exhibited full confluence in spontaneously contracting cultures. Sporadically observed quiescent cultures contained disarrayed and relatively atrophied cells and were not functionally assessed. The cells in isotropic cultures exhibited polymorphic shapes and random orientation on both micro (several cell lengths) and macro (mm to cm) length scales, followed by star-like patterns of polymerized actin fibers (Figure 3A). In contrast, cells on abraded cover slips attained an elongated spindle-like shape and preferential orientation in the direction of microabrasion (Figure 2B). Locally, the long cell axis varied around this direction, with a smaller deviation and higher degree of cell coalignment produced by coarser microabrasion (Figures 3C and 3E). Cell elongation in anisotropic cultures was associated with coalignment of actin fibers (Figure 2B) along the long cell axis, parallel arrangement of sarcomeres (Figure 2C), and elongation of cell nuclei (Figures 2B through 2D), similar to what has been found in native tissue. Membrane distribution of connexin43 was uniform and punctate both in isotropic (not shown) and in anisotropic cultures (Figure 2D), as is characteristic of neonatal cardiac myocytes.[6]

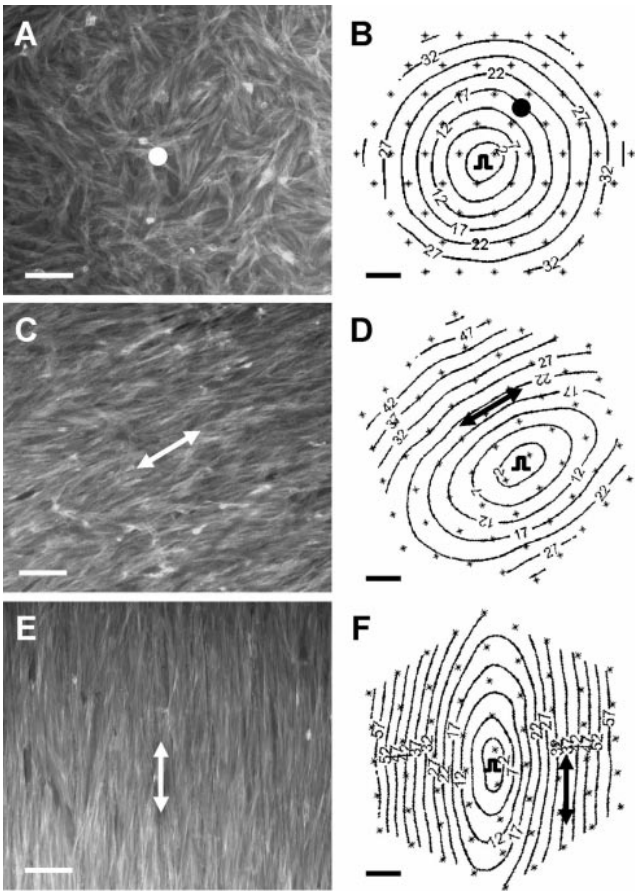

Figure 3. Structure-function relation in anisotropic cardiac cultures produced by microabrasion. Monolayer architecture shown using staining for actin fibers in isotropic (A), and anisotropic cultures grown on cover slips that were microabraded as fine (C) or coarse (E). A, C, and E, Bars=100 μm. Dots denote isotropic cultures with no abrasion. Double-headed arrows denote direction of abrasion and longitudinal fiber direction in anisotropic cultures. B, D, and F, Corresponding isochrones of electrical propagation at 5-ms intervals initiated by unipolar point stimulus at culture center (pulse symbol). Panels in each row are from the same monolayer, and all 3 monolayers are from the same harvest of cells. Numbers denote activation times in milliseconds relative to earliest activation. Crosses denote recording sites. B, D, and F, Bars=2 mm.

Oriented cell growth (Figures 3C and 3E) was followed by the fastest impulse propagation in the direction of abrasion (longitudinal direction). Figures 3B, 3D, and 3F show propagation in an isotropic and in 2 anisotropic cultures with longitudinal-to-transverse velocity ratios (ARs) of 1.7 and 3.0, produced by fine and coarse abrasion, respectively (also see online Movies 1 and 2, available online at http://www.circresaha.org in the data

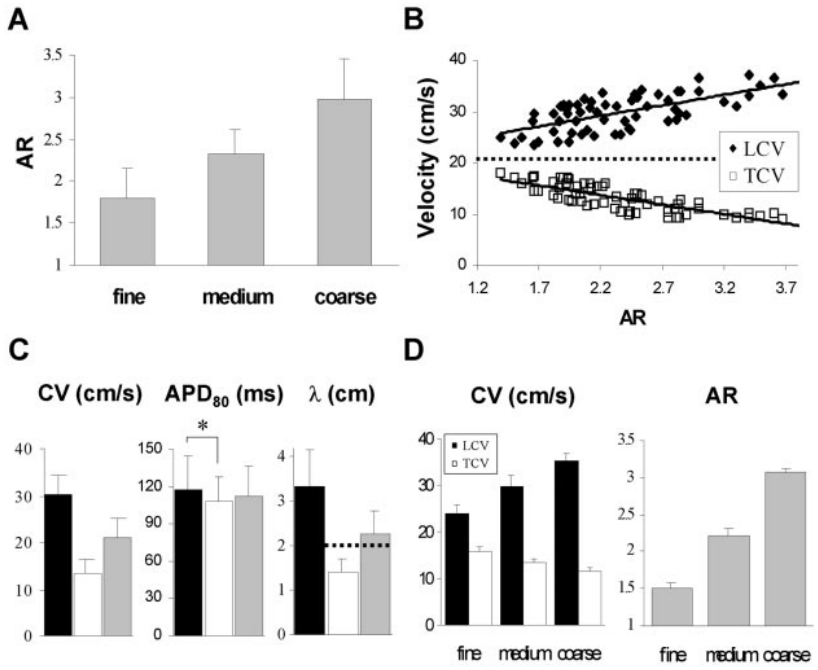

Figure 4. Electrophysiological parameters in anisotropic cardiac cultures produced by microabrasion. A, Anisotropy ratio (AR) in culture was increased by increasing coarseness of abrasion (n=20, 23, and 18 for fine, medium, and coarse abrasion, respectively). All groups differ significantly ($P<0.005$). B, Increase in AR was brought about by simultaneous increase in longitudinal (LCV), and decrease in transverse conduction velocity (TCV). Lines are linear fits to data with correlation coefficients $r=0.65$ and -0.82 for LCV and TCV, respectively. Dashed line is average CV for isotropic cultures. C, CV, APD_{80}, and wavelength ($\lambda=CV \cdot APD_{80}$) in longitudinal (black) and transverse (white) direction in anisotropic cultures (n=61) and in isotropic cultures (gray, n=12). All CVs and λs differ significantly from each other ($P<0.001$). *$P<0.05$, significantly different. Dashed line denotes diameter of monolayer culture (≈20 mm). D, CVs, and ARs in 3 cover slips produced using fine, medium, and coarse abrasion, respectively, that were used in n=4 consecutive cultures.

supplement). The corresponding circular and elliptical isochrones and velocity vector fields (not shown) revealed a uniform, smooth propagation throughout the cultures. Small microscopic clefts of subcellular or cellular size (up to 80 μm), observed only occasionally in the confluent cultures, did not interfere with the macroscopic spread of activation.

In 61 analyzed monolayers, AR ranged from 1.3 to 3.7 (2.34±0.59) with higher AR being produced by coarser abrasion (Figure 4A). Increase in AR due to cell elongation and coalignment resulted from both an increase in LCV (23.5 to 37.2 cm/s; $r=0.66$), and a decrease in TCV (18.1 to 9.2 cm/s; $r=-0.84$) (Figure 4B). Average conduction velocity for isotropic monolayers (21.2±3.7 cm/s, n=12, dashed line in Figure 4B) was intermediate between average values for TCV (13.4±2.7) and LCV (30.5±4.1) and is in agreement with previous studies for the same cell type in vitro[23] and ex vivo.[19] There was no significant correlation between APD_{80} and AR, so that the dependences of λ_L and λ_T on AR were similar to those of LCV and TCV, respectively (not shown). Figure 4C shows the averaged values for CV, APD, and λ from microabraded anisotropic and from isotropic cultures. $APD_{80,L}$ was slightly but significantly higher than $APD_{80,T}$ (117.7±27.4 versus 108.1±19.8 ms, respectively), which is consistent with previously published studies of the effect of anisotropic propagation on repolarization in canine and pig ventricles.[12,24] On average, the cover slip diameter (≈2 cm, dashed line in Figure 4C) was larger than λ_T (1.38±0.32 cm) and smaller than λ_L (3.35±0.79 cm). Microabraded cover slips that were reused in 4 consecutive cultures exhibited only small variations in LCV, TCV, and AR as shown in Figure 4D.

The direction of abrasion was systematically varied in adjacent areas of the same cover slip to produce sharp changes in cardiac fiber direction. Figure 5 shows staining for actin fibers in the vicinity of border zones (white dashed lines) located between adjacent isotropic (circle) and anisotropic (double arrow denoting longitudinal direction) portions of a monolayer (Figure 5A), and between adjacent areas where the direction of abrasion and consequently fiber direction were abruptly changed by 45° (Figure 5C) or 90° (Figure 5E). The entire border zone was sharp, with change in fiber direction occurring within several cell widths (≈50 to 100 μm) and without loss of cell confluence. As a functional consequence, the direction of fastest propagation of an electrical pulse abruptly changed when crossing the border zone between the two areas (Figures 5B, 5D, 5F, and online Movie 3). Application of 2× threshold (7±3 V/cm, n=9 monolayers) field stimuli during rest perpendicular to the border zone in cultures with 45° and 90° change in fiber direction, resulted in far-field activation that initiated along the border zone and subsequently propagated through the rest of the culture, as shown in the isochrone maps (Figures 5G, 5H, and online Movie 4).

Micropatterning

Fibronectin lines were successfully micropatterned throughout the entire cover slip surface. Figure 6A shows a cell monolayer (green stain for actin) that was deliberately scratched to expose the underlying fibronectin lines (stained in red). Cardiac cells attached and elongated on the fibronectin lines, bridged between the lines, and formed intercellular clefts. The cells exhibited alignment of actin fibers along the long cell axis (Figure 6B), parallel sarcomere organization (Figure 6C), elongation of cell nuclei (Figures 6B through 6D), and a punctate, random membrane distribution of connexin43 with no staining on the cleft borders (Figure 6D). Longitudinally oriented intercellular clefts (up to 1 mm long) were mostly acellular, or occasionally populated by noncardiomyocytes (white arrows in Figures 6B and 6C). Short, acellular longitudinal breaks in the patterned lines (up to 250 μm long) were only occasionally observed and resulted in extra wide (up to 80 μm) clefts. The extent of cell bridging between the adjacent cardiac fibers was directly proportional to the concentration of background fibronectin, which was

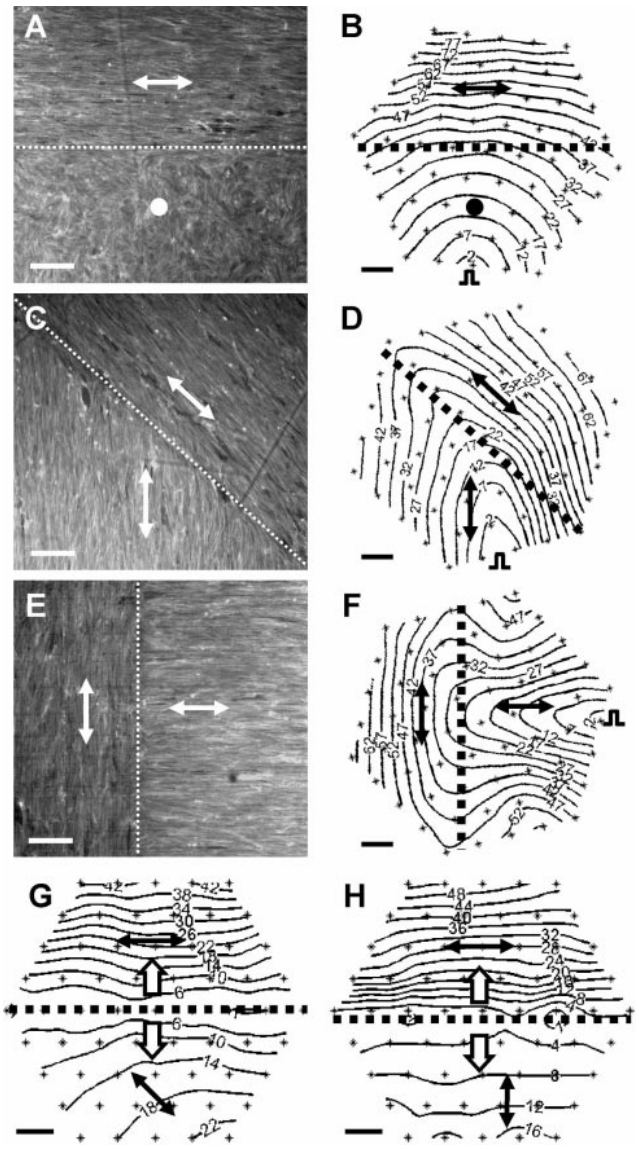

Figure 5. Structure-function relation in anisotropic cardiac cultures with change in fiber direction. Monolayer architecture (shown using actin staining) in the vicinity of the border zones (dashed lines) between isotropic and anisotropic portions of a monolayer (A), and between areas where direction of abrasion and consequently fiber direction were abruptly changed by 45° (C) and 90° (E), as shown by double-headed arrows. A, C, and E, Bars=200 μm. B, D, and F, Corresponding isochrones for A, C, and E, respectively, at 5-ms intervals after point stimulation at the edge of the cultures (pulse symbols). Field shock was applied during rest (diastole) using parallel platinum plates at 7.5 V/cm (2× threshold) in cultures with 45° (G) or 90° (H) change in fiber direction. Cathode plate is on top and anode plate on bottom, both at least 6 mm away from the edges of the monolayer, so that the field is oriented vertically. Block arrows denote direction of propagation. Isochrones are shown at 4-ms intervals. Note initial activation in the border zone (dashed line). Remaining nomenclature is as in Figure 3.

systematically increased to create a transition from microscopically discontinuous to continuous tissue architecture in the transverse direction, as shown using staining for actin (Figures 7A, 7C, and 7E). As a functional consequence of the increased number of transverse connections, the AR of electrical propagation decreased as shown in the isochrone maps in Figures 7B, 7D, and 7E (AR=5, 3.6, and 2, respectively) (see also online Movie 5 for an example of high AR).

Electrophysiological data (ARs, CVs, APDs, and λs) did not statistically differ between cultures with 12- and 25-μm wide fibronectin lines (with the same background fibronectin concentration) and were pooled together. In a total of 70 micropatterned monolayers, AR varied from 1.6 to 5.6 (3.4±1.0) with higher AR and lower TCV (not shown) being produced by lower concentrations of background fibronectin (Figure 8A). Application of the background fibronectin at concentrations greater than 10 μg/mL resulted in a disarray of the patterned cells, and an AR that was not statistically different from 1 (ie, cultures that were essentially isotropic; not shown). The increase in AR was primarily a consequence of a decrease in TCV (16.9 to 2.6 cm/s; $r=-0.95$) (Figure 4B). The LCV showed a slight but not significant increasing trend for AR <3.5 (22.8 to 38.7; $r=0.28$, $P=0.077$), and strong decreasing trend for AR >3.5 (36.4 to 14.6; $r=-0.85$, $P<0.0001$) (Figure 4B). Averaged APD_{80}, LCV, and λ_L in micropatterned cultures were comparable with those in microabraded cultures. However, averaged TCV (9.2±3.7 cm/s) and λ_T (0.94±0.42 cm) were significantly smaller than in microabraded cultures (compare with Figure 4C), because substantially lower values of TCV could be attained with micropatterning, which lowered the average value.

Discussion

We presented an in vitro model system that enables systematic control of the degree, orientation, and nonuniformity (continuity) of anisotropy in centimeter-sized monolayer cultures of neonatal rat cardiac myocytes. The use of cardiac cell networks with controlled anisotropic structure as a simplified model for optical mapping studies of functional cardiac electrophysiology offers several advantages over other established tissue preparations, including (1) tight, reproducible control of the cellular content and cell microenvironment, (2) elimination of the need for excitation-contraction decouplers that can alter the electrophysiological properties of cells,[25] and (3) certainty that the entire optical signal is produced only from a single layer of cells, thus enabling a one-to-one correspondence with 2-dimensional theoretical models and computer simulations.

Confluent anisotropic monolayers of cardiac myocytes have been previously used to study (1) the role of tissue discontinuities in microscopic impulse propagation,[15,26] or (2) the effect of extracellular matrix and external stretch on cell structure and protein turnover.[27,28] In those studies, cardiac cells were aligned on a thin collagen coat that was (1) gently rubbed by a fine brush after polymerization,[15] or (2) spread using a cell scraper and polymerized while slowly being poured within slightly tilted dishes.[27] Although the first approach has been shown to induce uniform anisotropy at only small (up to 2 mm) length scales, the second approach is difficult to apply when scaled down from a 10-cm culture dish to 2-cm diameter cover slip, which is a size that can be entirely optically mapped with reasonable spatial resolution. Our method offers several important advantages such as the following: (1) control over the shape of the substrate (PVC cover slip cut to specified shape); (2) systematic variation of the degree, uniformity, and continuity of anisotropy throughout the monolayer (Figures 2 to 4 and 6 to 8); (3) control over the fiber

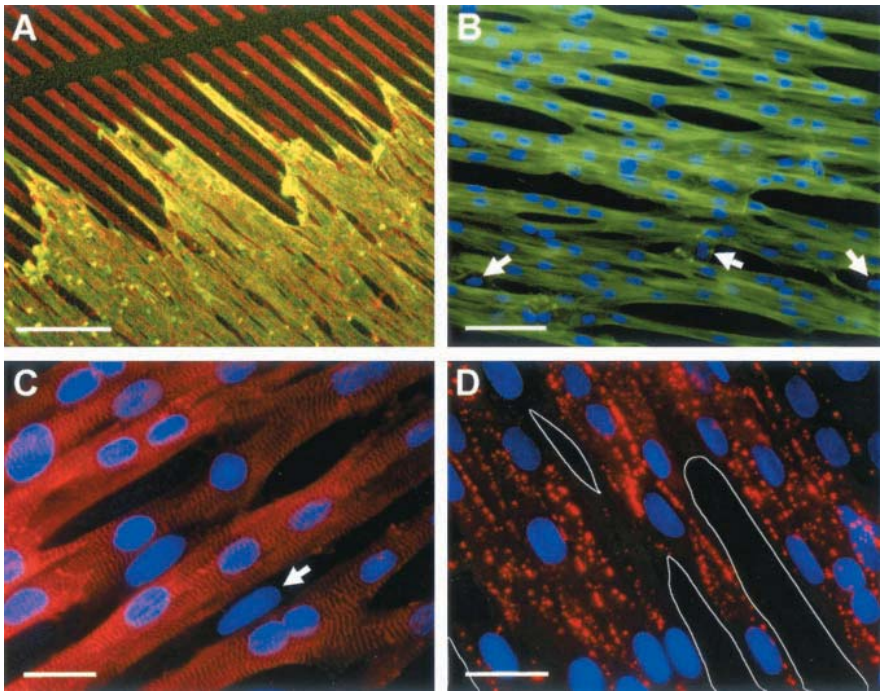

Figure 6. Cardiac cell morphology in anisotropic cultures produced by micropatterning. A, Monolayer was stained for actin (green) and fibronectin (red), and scratched using a thin needle to expose underlying fibronectin lines. Yellow shows where green and red overlap. Note longitudinal intercellular clefts (gaps in green staining) parallel to fibronectin lines. Concentration of background fibronectin was 1.25 μg/mL. Bar=200 μm. B, C, and D, Architecture of discontinuous micropatterned monolayer with no background fibronectin. Actin (B) is stained green, sarcomeric α-actinin (C) is red, connexin-43 (D) is red, and cell nuclei are blue. Arrows in B and C denote noncardiomyocytes. White lines in D indicate borders of intercellular clefts. B, Bar=100 μm. C and D, Bars=25 μm.

direction in adjacent regions of the same monolayer (Figure 5); and (4) better reproducibility, because the same abraded cover slips can be reused in different experiments with only slight variation in functional electrophysiological parameters (Figure 4D). The possibilities to use one or more extracellular matrix proteins (eg, fibronectin, laminin, and collagen) as a substrate for anisotropic cell growth, and to control the spatial distribution of continuous and discontinuous architecture in the same preparation, offers additional advantages for in vitro macroscopic studies of structure-function relationships in cardiac muscle.

Microabrasion and micropatterning were presented in this study as two complementary methodologies for the control of anisotropy in cardiac monolayers. The microabrasion method is simple, reproducible, and readily useable by any laboratory, while the micropatterning approach allows for a greater range of ARs and design of nonuniform discontinuous anisotropy, but at the cost of requiring a microfabrication facility and a far greater degree of effort. These advantages and disadvantages may lend one or the other to be the preferred method for the investigator.

Microabrasion

The thin submicron- and micron-scale abrasion grooves (Figure 2A) provided only subcellular cues for cell contact guidance and oriented growth and were not sufficiently wide or deep to entrap entire cells. Studies on alignment of rat dermal fibroblasts on surfaces with similar sized microgrooves showed that deeper microgrooves induced better cell coalignment,[29] which is consistent with our results for grooves produced by the different abrasion head sizes. However, microabrasion with a much coarser paper ($\approx$30-μm abrasion head) produced deeper, but wider and sparser, abrasion grooves that resulted in spatially nonuniform anisotropic architecture and irregular elliptical isochrones with relatively low AR (not shown). Therefore, although coarser abrasion increases cell coalignment and anisotropy (Figure 4A), the limit in AR occurs when the groove and/or intergroove widths and cell size become comparable (ie, cells start to span transversely across the single groove and/or in between the grooves).

Increased cell coalignment and elongation in microabraded cultures was accompanied by the simultaneous increase of LCV and decrease of TCV, and consequently, an increase in AR (Figures 3B, 3D, 3F, and 4B). Changes in cell morphology (in anisotropic versus isotropic cultures) had no apparent effect on the uniform membrane distribution of connexin43, similar to the findings of Fast et al.[26] The observed cell coalignment in conjunction with increased cell length-to-width ratio (elongation) resulted in the simultaneous but opposite changes in the number of gap junctions per unit length in the longitudinal and transverse directions and could account for the opposite trends in LCV and TCV found in this study (Figure 4B). The effects of change in cell morphology on the expression and/or conductance of gap junction channels, if present, may have additionally influenced the observed velocity trends.

In previous studies by Fast et al,[15] cardiac cultures grown on brushed collagen supported the anisotropic spread of electrical activity over microscopic distances (135 μm), with an average AR of 1.89. In our study, cardiac cultures produced by microabrasion exhibited maximum cell confluence with virtually no intercellular clefts, and supported a smooth, macroscopically continuous impulse propagation (Figure 3), and so-called uniform anisotropy[5] over centimeter-sized distances. The range of ARs (1.3 to 3.7) accomplished using microabrasion techniques encompasses ARs present in healthy adult ventricles from humans[30] and most animal species that are currently used for electrophysiological studies (ie, mouse,[31] guinea pig,[11] rat,[32] rabbit,[10] pig,[12] sheep,[33] and dog[24,34]). This study (Figures 2D and 6D) and other studies[6,26,34] have demonstrated that in neonatal cardiac cells, gap junctions distribute uniformly around the cell perimeter, whereas in adult cells, they predominantly localize at

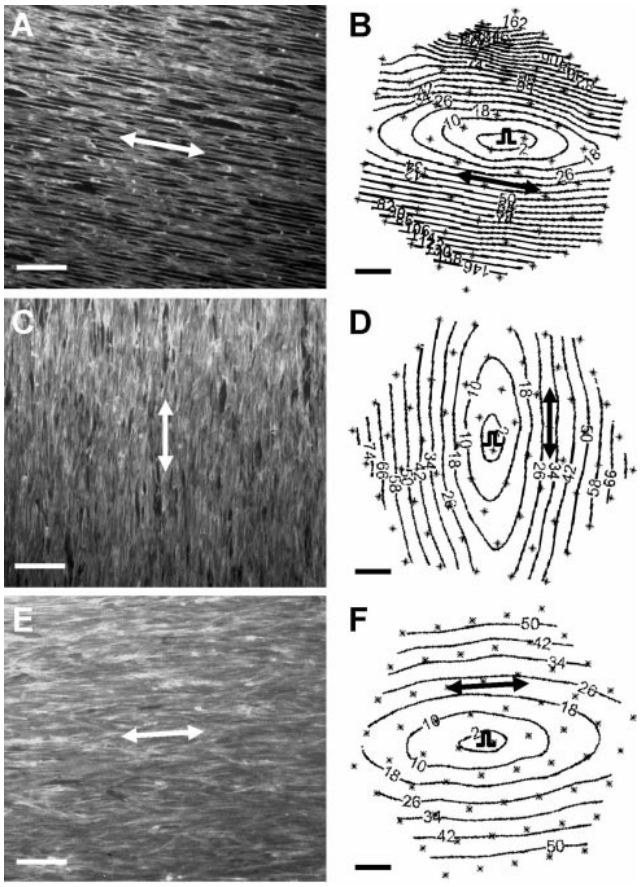

Figure 7. Structure-function relation in anisotropic cardiac cultures produced by micropatterning. Monolayer architecture is shown using actin staining in cultures with background fibronectin concentrations of 0 (A), 1.25 (C), and 5 (E) μg/mL. A, C, and E, Bars=250 μm. Double-headed arrows denote direction of micropatterned fibronectin lines and longitudinal fiber direction. Corresponding isochrones of electrical propagation initiated at center of monolayer (pulse symbol) are shown at 8-ms intervals. Note increased transverse conduction velocity in B, D, and F (3.9, 9.7, and 13.6 cm/s, respectively). Remaining nomenclature is as in Figure 3.

the cell ends (poles).[6,34] However, the degree of functional anisotropy in heart is governed not only by gap junction distribution but also by cell shape and size, as well as number and spatial distribution of neighboring cells (cell packing geometry).[1,34,35] In support of this concept, our results demonstrate that physiological ARs from adult ventricles can be attained solely by changing the coalignment and geometry of neonatal cardiomyocytes with uniformly distributed gap junctions. The average LCV and TCV values in our confluent anisotropic cultures are in excellent agreement with those reported for ventricles of neonatal rabbits[36] or neonatal dogs,[34] but are generally scaled down (1.2 to 2.2 times) compared with those measured in adult ventricles,[10,33,34] most likely due to the smaller cell size and lower gap junction conductance in neonatal versus adult cardiac cells.[34,37]

Besides uniform anisotropy, the microabrasion techniques were used to produce cardiac monolayer cultures with sharp, yet continuous (no intercellular clefts) changes in fiber direction (Figures 5A, 5C, and 5E), which resulted in abrupt changes in the longitudinal direction of impulse propagation (Figures 5B, 5D, and 5F). Adjacent regions with different anisotropies in the border zones of myocardial infarcts,[9] or areas with sharp changes in fiber direction,[7] have been shown to coincide spatially with sites of reentry. Moreover, the zone where fiber direction abruptly changes exhibits a sharp change in intracellular conductivity along a given direction and according to theoretical studies[2,3] can act as a site of far-field excitation during the defibrillation shock. Our observations of a field-induced initial depolarization along the entire border between areas with different fiber directions (Figures 5G and 5H) clearly validate the theoretical predictions.[2,3]

Micropatterning

The very high degrees of anisotropy (AR >4) observed in atria,[4] aged,[5] and fibrotic[38] cardiac tissue brought about by the presence of collagenous septa and decreased number of lateral (transverse) cell connections could not be achieved in confluent anisotropic cultures produced by microabrasion. A more sophisticated method of micropatterning was developed to systematically vary the amount of lateral connections while generally maintaining the cell elongation and orientation along the direction of micropatterned fibronectin lines. A decrease in the concentration of background fibronectin in these cultures resulted in the emergence of longitudinally oriented intercellular clefts and a gradual transition from continuous (Figure 7E) to discontinuous (Figure 7A) monolayer architecture that was accompanied by a decrease in effective TCV to values as low as 2.6 cm/s and an increase in AR to values as high as 5.6 (Figure 8B). As shown in theoretical studies by Pertsov,[39] the presence of tissue clefts results in an increase in macroscopic AR if cleft length is comparable to or larger than the width of the depolarization front, W, defined as the product between velocity and duration of action potential upstroke. For this study, W is estimated to be $\approx$0.3 mm/ms$\times$1 ms[26]=300 μm, which is comparable to or smaller than the cleft lengths encountered in micropatterned cultures with high ARs (Figure 7A).

Extremely high anisotropy (AR >6) observed during nonuniform anisotropic conduction in old and fibrotic hearts[5,38] could not be achieved in patterned neonatal cells, most likely because of their uniform gap junction distribution, and/or relatively small size (primarily length) of the intercellular clefts compared with that of collagenous septa in old or fibrotic tissue.[5,13] Although cleft size can be increased by increasing the spacing between patterned lines, or by inhibiting cell attachments between lines with the use of cell-repellant coatings (eg, bovine serum albumin on polystyrene[40]), the uniform gap junction distribution of neonatal cells may still remain a limiting factor in obtaining extremely high ARs in micropatterned cultures.

Interestingly, an increase in the degree of transverse discontinuity (for AR >3.5) in micropatterned cultures resulted not only in the expected decrease of transverse velocity, but also in a decrease of macroscopic longitudinal velocity (Figure 8B), which might arise from repetitive conduction slowings at sites of interfiber connections, similar to results from studies on microscopic propagation in branched cell strands.[17] Alternatively, the spindle-like shape and uniform gap junction distribution of neonatal myocytes may augment the role of lateral gap junctions in longitudinal propagation, and yield progressive longitudinal

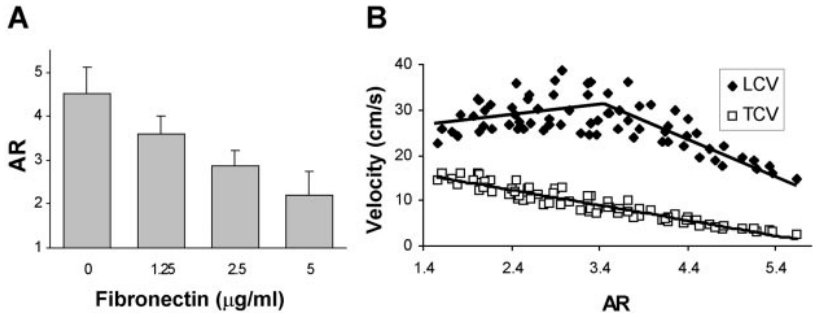

Figure 8. Electrophysiological parameters in anisotropic cardiac cultures produced by micropatterning. A, Anisotropy ratio (AR) in culture was increased by decreasing the concentration of background fibronectin (n=15, 20, 20, and 15 for 0, 1.25, 2.5, and 5 μg/mL, respectively). All groups differ significantly ($P<0.001$). B, Increase in AR was brought about by decrease in TCV. Lines are linear fits to data with correlation coefficients of $r=-0.95$, 0.28 (NS, $P=0.077$) for TCV, LCV (for AR <3.5), respectively, and $r=-0.85$ for LCV (for AR >3.5).

slowing with increase in transverse decoupling. In contrast, transverse decoupling in adult cardiac tissue may only marginally affect longitudinal velocity due to the rod cell shape and polar distribution of gap junctions in adult cells. Nevertheless, the increased anisotropy and slowed conduction in discontinuous micropatterned cultures should enhance their propensity for reentrant cardiac arrhythmias.[41]

Despite the structural and functional differences from intact adult cardiac muscle (eg, 2-dimensionality, cell geometry, gap junction distribution, and conduction velocity), a cardiac cell culture system that combines control over tissue composition, structure, and function with optical mapping at a macroscopic length scale appears well-suited for studies of impulse propagation and dynamics of reentrant cardiac arrhythmias in a 2-dimensional in vitro setting. Our recent studies on mechanisms of reentry acceleration in uniformly anisotropic cardiomyocyte cultures[42,43] support this concept.

Acknowledgments

This work was supported by NIH grant HL66239 and a Grant-in-Aid from the Mid-Atlantic Affiliate of the American Heart Association to L.T., NIH training grant HL07581 support of K.K.P., and an American Heart Association, Mid-Atlantic Affiliate fellowship to N.B. We are grateful to Chae-Ryon Kong and Gaddum Duemani Reddy for their assistance with the optical mapping system, and Dr Chris Chen and John Tan for their advice on micropatterning.

References

1. Saffitz JA, Kanter HL, Green KG, Tolley TK, Beyer EC. Tissue-specific determinants of anisotropic conduction velocity in canine atrial and ventricular myocardium. *Circ Res*. 1994;74:1065–1070.
2. Sobie EA, Susil RC, Tung L. A generalized activating function for predicting virtual electrodes in cardiac tissue. *Biophys J*. 1997;73:1410–1423.
3. Trayanova N, Skouibine K, Aguel F. The role of cardiac tissue structure in defibrillation. *Chaos*. 1998;8:221–233.
4. Koura T, Hara M, Takeuchi S, Kenichi O, Okada Y, Miyoshi S, Watanabe A, Shiraiwa K, Mitamura H, Kodama I, Ogawa S. Anisotropic conduction properties in canine atria analyzed by high-resolution optical mapping: preferential direction of conduction block changes from longitudinal to transverse with increasing age. *Circulation*. 2002;105:2092–2098.
5. Spach MS, Dolber PC. Relating the extracellular potentials and their derivatives to anisotropic propagation at a microscopic level in human cardiac muscle. Evidence for electrical uncoupling of side-side fiber connections with increasing age. *Circ Res*. 1986;58:356–371.
6. van Kempen MJA, Fromaget C, Gros D, Moorman AF, Lamers WH. Spatial distribution of connexin-43, the major cardiac gap junction protein in the developing and adult rat heart. *Circ Res*. 1991;68:1638–1651.
7. Valderrabano M, Lee MH, Ohara T, Lai AC, Fishbein MC, Lin SF, Karagueuzian HS, Chen PS. Dynamics of intermural and transmural reentry during ventricular fibrillation in isolated swine ventricles. *Circ Res*. 2001;88:839–848.
8. Carey PA, Turner M, Fry CH, Sheridan DJ. Reduced anisotropy of action potential conduction in left ventricular hypertrophy. *J Cardiovasc Electrophysiol*. 2001;12:830–835.
9. Peters NS, Wit AL. Myocardial architecture and ventricular arrhythmogenesis. *Circulation*. 1997;97:1746–1754.
10. Boersma L, Brugada J, Kirchhof C, Allessie M. Mapping of reset of anatomic and functional reentry in anisotropic rabbit ventricular myocardium. *Circulation*. 1994;89:852–862.
11. Girouard SD, Pastore JM, Laurita KR, Gregory KW, Rosenbaum DS. Optical mapping in a new guinea pig model of ventricular tachycardia reveals mechanisms for multiple wavelengths in a single reentrant circuit. *Circulation*. 1996;93:603–613.
12. Gotoh M, Uchida T, Fan W, Fishbein MC, Karagueuzian HS, Chen PS. Anisotropic repolarization in ventricular tissue. *Am J Physiol*. 1997;272:H107–H113.
13. Kawara T, Derksen R, de Groot JR, Coronel R, Tasseron S, Linnenbank AC, Hauer RNW, Kirkels H, Janse MJ, de Bakker JMT. Activation delay after premature stimulation in chronically diseased human myocardium relates to the architecture of interstitial fibrosis. *Circulation*. 2001;104:3069–3075.
14. Rohr S, Sholly DM, Kleber AG. Patterned growth of neonatal rat heart cells in culture: morphological and electrophysiological characterization. *Circ Res*. 1991;68:114–130.
15. Fast VG, Kleber AG. Anisotropic conduction in monolayers of neonatal rat heart cells cultured on collagen substrate. *Circ Res*. 1994;75:591–595.
16. Fast VG, Rohr S, Gillis AM, Kleber AG. Activation of cardiac tissue by extracellular electrical shocks: formation of "secondary sources" at intracellular clefts in monolayers of cultured myocytes. *Circ Res*. 1998;82:375–385.
17. Kucera JP, Kleber AG, Rohr S. Slow conduction in cardiac tissue, II. Effects of branching tissue geometry. *Circ Res*. 1998;83:795–805.
18. Entcheva E, Lu SN, Troppman RH, Sharma V, Tung L. Contact fluorescent imaging of reentry in monolayers of cultured neonatal rat ventricular myocytes. *J Cardiovasc Electrophysiol*. 2000;11:665–676.
19. Bursac N, Papadaki M, Cohen RJ, Schoen FJ, Eisenberg SR, Carrier R, Vunjak-Novakovic G, Freed LE. Cardiac muscle tissue engineering: towards an in vitro model for electrophysiological studies. *Am J Physiol*. 1999;277:H433–H444.
20. Whitesides GM, Ostuni E, Takayama S, Jiang X, Ingber DE. Soft lithography in biology and biochemistry. *Annu Rev Biomed Eng*. 2001;3:335–373.
21. Tan JL, Tien J, Chen S. Microcontact printing of proteins on mixed self-assembled monolayers. *Langmuir*. 2002;18:519–523.
22. Parker KK, Brock AL, Brangwynne C, Mannix RJ, Wang N, Ostuni E, Geisse NA, Adams JC, Whitesides GM, Ingber DE. Directional control of lamellipodia extension by constraining cell shape and orienting cell tractional forces. *FASEB J*. 2002;16:1195–1204.
23. Meiry G, Reisner Y, Feld Y, Goldberg S, Rosen M, Ziv N, Binah O. Evolution of action potential propagation and repolarization in cultured neonatal rat ventricular myocytes. *J Cardiovasc Electrophysiol*. 2001;12:1269–1277.
24. Osaka T, Kodama I, Tsuboi N, Toyama J, Yamada K. Effects of activation sequence and anisotropic cellular geometry on the repolarization phase of action potential of dog ventricular muscles. *Circulation*. 1987;76:226–236.
25. Lee MH, Lin SF, Ohara T, Omichi C, Okuyama Y, Chudin E, Garfinkel A, Weiss JN, Karagueuzian HS, Chen PS. Effects of diacetyl monoxime and cytochalasin D on ventricular fibrillation in swine right ventricles. *Am J Physiol*. 2001;280:H2689–H2696.
26. Fast VG, Darrow BJ, Saffitz JE, Kleber AG. Anisotropic activation spread in heart cell monolayers assessed by high-resolution optical mapping: role of tissue discontinuities. *Circ Res*. 1996;79:115–127.
27. Simpson DG, Terracio L, Terracio M, Price RL, Turner DC, Borg TK. Modulation of cardiac myocyte phenotype in vitro by the composition and orientation of the extracellular matrix. *J Cell Physiol*. 1994;161:89–105.

28. Simpson DG, Majeski M, Borg TK, Terracio L. Regulation of cardiac myocyte protein turnover and myofibrillar structure in vitro by specific directions of stretch. *Circ Res*. 1999;85:e59–e69.
29. Walboomers XF, Monaghan W, Curtis ASG, Jansen JA. Attachment of fibroblasts on smooth and microgrooved polystyrene. *J Biomed Mat Res*. 1999;46:212–220.
30. Taggart P, Sutton PI, Opthof T, Coronel R, Trimlett R, Pugsley W, Kallis P. Inhomogeneous transmural conduction during early ischaemia in patients with coronary artery disease. *J Mol Cell Cardiol*. 2000;32:621–630.
31. Vaidya D, Morley GE, Samie FH, Jalife J. Reentry and fibrillation in the mouse heart: a challenge to the critical mass hypothesis. *Circ Res*. 1999;85:174–181.
32. Sun LS, Legato MJ, Rosen TS, Steinberg SF, Rosen MR. Sympathetic innervation modulates ventricular impulse propagation and repolarization in immature rat heart. *Cardiovasc Res*. 1993;27:459–463.
33. Zaitsev AV, Berenfeld O, Mironov SF, Jalife J, Pertsov AM. Distribution of excitation frequencies on the epicardial and endocardial surfaces of fibrillating ventricular wall of sheep heart. *Circ Res*. 2000;86:408–417.
34. Spach MS, Heidlage JF, Dolber PC, Barr RC. Electrophysiological effects of remodeling cardiac gap junctions and cell size: experimental and model studies of normal cardiac growth. *Circ Res*. 2000;86:302–311.
35. Jongsma HJ, Wilders R. Gap junctions in cardiovascular disease. *Circ Res*. 2000;86:1193–1197.
36. Litchenberg WH, Norman LW, Holwell AK, Martin KL, Hewett KW, Gourdie RG. The rate and anisotropy of impulse propagation in the postnatal terminal crest are correlated with remodeling of Cx43 gap junction pattern. *Cardiovasc Res*. 2000;45:379–387.
37. Fishman GI, Hertzberg EL, Spray DC, Leinwand LA. Expression of connexin43 in the developing rat heart. *Circ Res*. 1991;68:782–787.
38. de Bakker JMT, van Cappele FJL, Janse MJ. Slow conduction in the infarcted human heart: 'zigzag' course of activation. *Circulation*. 1993;88:915–926.
39. Pertsov AM. Scale of geometric structures responsible for discontinuous propagation in myocardial tissue. In: Spooner P, Joyner R, Jalife J, eds. *Discontinuous Conduction in the Heart*. New York, NY: Futura; 1997:273–293.
40. McDevitt TC, Angello JC, Whitney ML, Reinecke H, Hauschka SD, Murry CE, Stayton PS. In vitro generation of differentiated cardiac myofibers on micropatterned laminin surfaces. *J Biomed Mat Res*. 2002;60:472–479.
41. Spach MS, Josephson ME. Initiating reentry: the role of nonuniform anisotropy in small circuits. *J Cardiovasc Electrophysiol*. 1994;5:182–209.
42. Bursac N, Iravanian S, Parker KK, Tung L. Anisotropic reentry in cultures of cardiac myocytes. *PACE*. 2002;25:578. Abstract.
43. Bursac N, Tung L. Novel stable functional reentrant patterns induced by rapid pacing in uniformly anisotropic cardiomyocyte cultures. *Circulation*. 2002; 106:II-304.

The animations of electrical propagation were generated from signals that were band-pass filtered between 5 and 15 Hz.

Movie 1. Propagation in an isotropic culture, initiated by point stimuli at center.

Movie 2. Propagation in an anisotropic culture produced by microabrasion, initiated by point stimuli at center.

Movie 3. Propagation in a culture with 90 degree change in fiber orientation (see Figs 5E, 5F) initated by point stimuli at periphery.

Movie 4. Propagation initiated by a field stimulus in a culture with 90 degree change in fiber orientation (see Figs 5E, 5H).

Movie 5. Propagation in an anisotropic culture produced by micropatterning, initiated by point stimuli at center.